Nonlinear GN model for coherent optical communications systems with hybrid fiber spans

I. Roudas

Electrical and Computer Engineering
Montana State University
Bozeman, MT 59717, USA
ioannis.roudas@montana.edu

X. Jiang

Engineering and Environmental Science
College of Staten Island
City University of New York
Staten Island, NY 10314, USA
jessica.jiang@csi.cuny.edu

J. Kwapisz Mathematical Sciences Montana State University Bozeman, MT 59717, USA

jarek@math.montana.edu

Abstract—The nonlinear Gaussian-noise (GN) model is a useful analytical tool for the estimation of the impact of distortion due to Kerr nonlinearity on the performance of coherent optical communications systems with no inline dispersion compensation.

The original nonlinear GN model was formulated for coherent optical communications systems with identical single-mode fiber spans. Since its inception, the original GN model has been modified for a variety of link configurations. However, its application to coherent optical communications systems with hybrid fiber spans, each composed of multiple fiber segments with different attributes, has attracted scarcely any attention.

This invited paper is dedicated to the extended nonlinear GN model for coherent optical communications systems with hybrid fiber spans. We review the few publications on the topic and provide a unified formalism for the analytical calculation of the nonlinear noise variance.

To illustrate the usefulness of the extended nonlinear GN model, we apply it to coherent optical communications systems with fiber spans composed of a quasi-single-mode fiber segment and a single-mode fiber segment in tandem. In this configuration, a quasi-single-mode fiber with large effective area is placed at the beginning of each span, to reduce most of the nonlinear distortion, followed by a single-mode fiber segment with smaller effective-area, to limit the multipath interference introduced by the quasi-single-mode fiber to acceptable levels. We show that the optimal fiber splitting ratio per span can be calculated with sufficient accuracy using the extended nonlinear GN model for hybrid fiber spans presented here.

Index Terms—Nonlinear Gaussian-noise (GN) model, coherent optical communications systems, hybrid fiber spans.

I. Introduction

Modeling of the fiber nonlinearities has been the cornerstone of optical communications theoretical research since the early days of the field [1]. The one-dimensional, scalar nonlinear Schrödinger equation [1] and its vector counterpart, the Manakov equation [2], that govern the propagation of optical waveforms in optical fibers, have been intensively studied for direct-detection and coherent optical communications systems [1]. In particular, over the last decade, there has been considerable progress in finding approximate analytical solutions of these equations for coherent optical communications systems with no inline dispersion compensation, e.g., [3]–[14].

The conventional nonlinear Gaussian-noise (GN) model [5]–[7], [9] has gained popularity over time due to its relative

simplicity compared to other, more accurate but more elaborate mathematical formulations [10], [11]. According to the nonlinear GN model, signal distortion due to Kerr nonlinearity can be represented by a zero-mean, complex Gaussian additive noise. The variance of the latter is calculated in a closed-form from fiber and system parameters [7], [9].

Since its inception, the original nonlinear GN model has been constantly refined, e.g., [12], and has been modified for a variety of link configurations, e.g., [15], and most recently, e.g., [16], [17]. However, to the best of our knowledge, its application to coherent optical communications systems with hybrid fiber spans composed of multiple fiber segments of different fiber types has hardly received any attention to date. Notable exceptions are the papers [18], [19] devoted to quasi-single-mode fibers, as well as more recent publications focusing on optical phase conjugation [20] and on discrete Raman amplification [21].

This invited paper is dedicated to the extended nonlinear GN model for coherent optical communications systems with hybrid fiber spans. In the first part of the paper, we review the few publications on the topic and provide a unified formalism for the analytical calculation of the nonlinear noise variance. In the second part of the paper, we apply the proposed model to coherent optical communications systems with fiber spans composed of quasi-single-mode fiber and single-mode fiber segments. We show that the optimal fiber splitting ratio per span can be calculated with sufficient accuracy using the extended nonlinear GN model for hybrid fiber spans presented here.

II. ANALYTICAL MODEL

A. System topology

Consider a long-haul coherent optical communications system with no inline dispersion compensation. The system is composed of N_s identical fiber spans of length ℓ_s each. There are N_f fiber types per span with lengths ℓ_{s_k} , where $k=1,\ldots,N_f$. The k-th fiber segment in each span is characterized by its attenuation coefficient a_k , its group velocity dispersion (GVD) parameter β_{2_k} , and its nonlinear coefficient γ_k . The attributes of each fiber segment are constant along its length. Different fiber segments have different fiber attributes.

At the end of each fiber span, there is a lumped optical amplifier of gain G equal to the span loss and noise figure F_A .

We consider wavelength division multiplexing (WDM) and polarization division multiplexing (PDM) based on ideal Nyquist channel spectra. The latter are created using squareroot raised-cosine filters with approximately zero roll-off factor at the transmitter and the receiver. Furthermore, without loss of generality, we assume that a WDM PDM optical signal is composed of an odd number N_{ch} wavelength channels with spacing $\Delta \nu \simeq R_s$, where R_s is the symbol rate. The optical bandwidth of the transmitted signal is $B_0 = N_{ch}R_s$. We denote by P the total average launch power per channel (in both polarizations). We want to evaluate the performance of the center WDM PDM channel at wavelength λ .

B. Effective optical signal-to-noise ratio

The performance of coherent optical systems without in-line chromatic dispersion compensation is related to the *effective* optical signal-to-noise ratio (OSNR_{eff}) at the receiver input. This quantity takes into account the amplified spontaneous emission (ASE) noise, the crosstalk, and the nonlinear distortion. For engineering purposes, we assume that all the above effects can be modeled as independent, zero-mean, complex Gaussian noises. More specifically, the OSNR_{eff} measured at a resolution bandwidth $\Delta\nu_{\rm res}$ can be well described by the analytical relationship [6], [22]

$$OSNR_{eff} = \frac{P}{\tilde{a} + \tilde{\beta}P + \tilde{\gamma}P^3},\tag{1}$$

where \tilde{a} is the ASE noise variance, $\tilde{\beta}P$ is the crosstalk variance, and $\tilde{\gamma}P^3$ is the nonlinear noise variance. The coefficients $\tilde{a}, \tilde{\beta}$, and $\tilde{\gamma}$ depend on fiber and system parameters.

C. Nonlinear noise variance

For coherent optical communications systems with hybrid fiber spans, the nonlinear noise coefficient is given by the double integral

$$\tilde{\gamma} \simeq \frac{16}{27} \frac{N_s^2 \Delta \nu_{\text{res}}}{R_s^3} \int_{-B_0/2}^{B_0/2} \int_{-B_0/2}^{B_0/2} \xi(f_1, f_2) \, df_1 df_2. \tag{2}$$

Expression (2) is similar to the nonlinear GN formula eq. (18) in [6] for a single fiber type per span. The integrand $\xi(f_1, f_2)$ is written as a product of a four-wave mixing efficiency term $\eta(f_1, f_2)$ and a phased-array term $\phi(f_1, f_2)$

$$\xi(f_1, f_2) := \eta(f_1, f_2) \phi(f_1, f_2).$$
 (3)

The four-wave mixing efficiency per span is

$$\eta(f_1, f_2) \coloneqq \left| \sum_{k=1}^{N_f} \hat{\gamma}_k(f_1, f_2) \, \hat{L}_{\text{eff}_k}(f_1, f_2) \right|^2,$$
(4)

where $\hat{\gamma}_k(f_1, f_2)$ are the complex nonlinear fiber coefficients

$$\hat{\gamma}_k(f_1, f_2) := \gamma_k e^{-\sum_{m=1}^{k-1} \alpha_m(f_1, f_2)\ell_{s_m}}, \tag{5}$$

and $\hat{L}_{\text{eff}_k}(f_1, f_2)$ are the complex effective lengths, defined as

$$\hat{L}_{\text{eff}_k}(f_1, f_2) := \frac{1 - e^{-\alpha_k(f_1, f_2)\ell_{s_k}}}{\alpha_k(f_1, f_2)}.$$
 (6)

The introduction of the complex nonlinear fiber coefficients $\hat{\gamma}_k$ and the complex effective lengths \hat{L}_{eff_k} provides a convenient mnemonic rule since the four-wave mixing efficiency per span $\eta\left(f_1,f_2\right)$ is expressed in terms of a simple weighted sum (14) of the complex nonlinear coefficients (5) times the normalized complex effective lengths (6) of the different fiber segments.

In (5), (6), we have defined the complex attenuation coefficients as

$$\alpha_k(f_1, f_2) := a_k + i\Delta\beta_k(f_1, f_2),\tag{7}$$

where $\Delta \beta_k(f_1, f_2)$ denote the propagation constant mismatches for different fiber segments in each span,

$$\Delta \beta_k(f_1, f_2) := -4\pi^2 \beta_{2k} f_1 f_2. \tag{8}$$

The coherent addition of the contributions of successive fiber spans to the total nonlinear noise leads to a phased-array term $\phi(f_1, f_2)$, as in the original nonlinear GN model [7], [9]. The difference is that, in the hybrid fiber span case, the phased-array term depends on the average phase mismatch (10) of all optical fibers per span. More specifically, the normalized phased-array term in (3) is defined as

$$\phi(f_1, f_2) := \frac{1}{N_s^2} \frac{\sin^2 \left[N_s \Delta \beta(f_1, f_2) \,\ell_s / 2 \right]}{\sin^2 \left[\Delta \beta(f_1, f_2) \,\ell_s / 2 \right]}, \tag{9}$$

where $\Delta\beta(f_1,f_2)$ is the average propagation constant mismatch

$$\Delta\beta(f_1, f_2) := \ell_s^{-1} \sum_{k=1}^{N_f} \Delta\beta_k(f_1, f_2) \ell_{s_k}.$$
 (10)

To simplify the calculation of (2), we can substitute $N_s^{1+\epsilon}$ for $N_s^2\phi(f_1,f_2)$, where ϵ is a fitting constant [7]. The case $\epsilon \neq 0$ corresponds to partially-coherent addition of the contributions of successive fiber spans to the total nonlinear noise. For $\epsilon=0$, nonlinear noises from different spans add incoherently.

D. Literature review

Formulae (2)-(10) were derived assuming that the fiber parameters a, β_2 , and γ are piecewise functions of the propagation distance. While the formalism presented here is most general, previous publications studied important special cases where one or more of the aforementioned fiber parameters were allowed to vary along the link length. For instance, Shieh and Chen [4] examined the case of multi-segment fiber spans composed of a transmission fiber followed by a dispersion compensating fiber (DCF) sandwiched between two EDFAs. Furthermore, the nonlinear GN model formalism proposed by Curri et al. [15] for Nyquist-WDM coherent optical systems using Raman amplification contained a general theoretical framework that could be potentially exploited for the analysis of nonlinear accumulation in systems with multiple fiber segments per span (not necessarily comprising Raman amplifiers).

Independently, Downie et al.[18, Section IV] and Miranda et al. [19] extended the conventional Gaussian noise model to the performance evaluation of coherent optical communication systems with hybrid fiber spans composed of quasi-singlemode fibers (QSMFs) and single-mode fibers (SMFs). In parallel, Al-Khateeb et al. [20, equation (4)] derived almost identical expressions to (2)-(10) for distributed Raman systems. A minor difference is that all fiber segments in [20, equation (4)] have the same nonlinear coefficient γ . Most recently, Krzczanowicz at el. [21] published an analytical formula for the nonlinear noise accumulation in optical communications systems using discrete Raman amplifiers, which is reminiscent of the formula of [19] derived in a different context. In conclusion, the analytical model presented in this paper cannot claim to be fundamentally new but is rather a synthesis of formalisms from previous publications.

E. Computing the nonlinear noise coefficient

For computational convenience, the double integral (2) can be converted into a single integral by using a transformation of integration variables.

To begin, since ξ (f_1 , f_2) is an even function of f_1 , f_2 , we can reduce the region of integration to the upper right quadrant of the coordinate plane

$$\tilde{\gamma} = \frac{64}{27} \frac{N_s^2 \Delta \nu_{\text{res}}}{R_s^3} \int_0^{B_0/2} \int_0^{B_0/2} \xi(f_1, f_2) \, df_1 df_2. \tag{11}$$

The integrand $\xi\left(f_1,f_2\right)$ depends only on the product of the integration variables f_1f_2 so it is beneficial to define a new integration variable $\zeta \coloneqq f_1f_2/2f_\phi^2$, where f_ϕ is the average phased-array bandwidth [3] $f_\phi^{-1} \coloneqq 2\pi\sqrt{|\beta_2|}\,\ell_s$, and β_2 is the average GVD parameter $\beta_2 \coloneqq \ell_s^{-1}\sum_{k=1}^{N_f}\beta_{2k}\ell_{sk}$. By changing the integration variables from f_1,f_2 to $f_1,\zeta,$

By changing the integration variables from f_1, f_2 to f_1, ζ , and using iterated integration, the double integral can be transformed into a single-integral

$$\tilde{\gamma} = \kappa \int_0^{\zeta_0} \ln\left(\frac{\zeta_0}{\zeta}\right) \xi\left(\zeta\right) d\zeta, \tag{12}$$

where we defined

$$\kappa \coloneqq \frac{128}{27} \frac{f_{\phi}^2}{R_s^2} N_s^2, \zeta_0 \coloneqq \frac{B_0^2}{8f_s^2}.$$
 (13)

The integrand $\xi(\zeta)$ is written as $\xi(\zeta) = \eta(\zeta) \phi(\zeta)$, where

$$\eta\left(\zeta\right) \coloneqq \left|\sum_{k=1}^{N_f} \hat{\gamma}_k\left(\zeta\right) \hat{L}_{\mathrm{eff}_k}\left(\zeta\right)\right|^2,\tag{14}$$

$$\phi\left(\zeta\right) \coloneqq \frac{1}{N_s^2} \frac{\sin^2(N_s \zeta)}{\sin^2(\zeta)}.\tag{15}$$

The final integral (12) is an improper integral of the second kind (i.e., the integrand becomes infinite at the lower end of the integration interval).

In order to evaluate this integral, we split the integration interval into two sub-intervals, $[0, \delta]$ and $[\delta, \zeta_0]$, where δ is in the vicinity of $\zeta = 0$.

For the first sub-interval, $[0, \delta]$, taking the Taylor expansion of the integrand and integrating by parts, we obtain the following expression

$$\int_{0}^{\delta} \ln\left(\frac{\zeta_{0}}{\zeta}\right) \xi(\zeta) d\zeta = \ln\left(\frac{\zeta_{0}}{\delta}\right) \int_{0}^{\delta} \xi(\zeta) d\zeta + \sum_{k=0}^{\infty} \frac{\delta^{k+1}}{k!(k+1)^{2}} \partial_{\zeta}^{k} \xi(0)$$
(16)

We can evaluate δ in (16) by imposing the condition that the zeroth-order term of the Taylor series in (16) should be much larger than the subsequent terms so that we can truncate the Taylor series to the zeroth-order term. This condition yields $\delta \ll 3\sqrt{3}/N_s$ for $N_s \gg 1$.

In the second sub-interval, $[\delta, \zeta_0]$, the integrand $\xi(\zeta)$ is oscillatory, mainly due to the phased-array term $\phi(\zeta)$. The latter is a periodic function with period π . Principal maxima of unit height occur at integer multiples of π . Between consecutive principal maxima (i.e., over a range of π) there are N_s-1 minima at multiples of π/N_s and N_s-2 subsidiary maxima approximately midway between successive minima.

To properly sample the oscillatory integrand, we resort to Simpson's quadrature. The integration interval can be subdivided into subintervals of width π/N_s . We sample each subinterval N_n times. Therefore, the distance between adjacent nodes is $\Delta = \pi/(N_s N_n)$.

Since the four-wave mixing efficiency $\eta\left(\zeta\right)$ becomes negligible for large values of ζ , to accelerate the numerical computation, we can limit the integration interval to $[\delta,\mu]$, $\mu\leq\zeta_0$, $\mu=(M+1)\pi$, where M is a natural number. The truncation error is bounded by

$$\int_{\mu}^{\zeta_0} \ln\left(\frac{\zeta_0}{\zeta}\right) \xi(\zeta) d\zeta \le \Gamma^2 \frac{1}{M\pi} \ln\left(\frac{\zeta_0}{M\pi}\right)$$
 (17)

where Γ is defined as

$$\Gamma := \sum_{k=1}^{N_f} \gamma_k \frac{\ell_{s_k}}{\lambda_k} e^{-\sum_{m=1}^{k-1} 2\lambda_m \sigma} \frac{1 + e^{-2\lambda_k \sigma}}{2}, \quad (18)$$

and we used several auxiliary quantities defined as $\sigma_k := \frac{1}{2} \frac{|\beta_2|}{|\beta_{2_k}|} a_k \ell_s$, $\lambda_k = \frac{|\beta_{2_k}|}{|\beta_2|} \frac{\ell_{s_k}}{\ell_s}$, $\sigma \coloneqq \min\{\sigma_k : k = 1, \dots, N_f\}$.

III. RESULTS AND DISCUSSION

In this section, we focus our attention on the optimal design of a typical transatlantic coherent optical communications system with hybrid fiber spans composed of an experimental QSMF [23], [24] and a commercially-available, ultra-low-loss, large-effective-area SMF without any splice losses. We evaluate, both analytically and numerically, the performance of various fiber configurations per span. We check the agreement between the analytical model of the previous section and Monte Carlo simulation, and we show that the proposed GN model is sufficient for the determination of the optimum fiber splitting ratio.

A. System parameters

We assume that the point-to-point link has total length equal to 6,000 km and is composed of 100 km spans. Furthermore, we assume an ideal Nyquist WDM signal composed of 9 wavelength channels, each carrying 32 GBd PDM 16-QAM. The attenuation coefficient of the QSMF is 0.16 dB/km and of the SMF is 0.158 dB/km. The effective mode area of the fundamental mode for the QSMF is 250 μ m² and of the SMF is 112 μ m². The GVD parameter β_2 is -26.6 ps²/km for both fiber types. The EDFA noise figure is 5 dB.

Launching light in the fundamental mode of an ideal, straight, perfectly-cylindrical QSMF results, in theory, in pure single-mode propagation without coupling to higherorder modes. In practice, however, there always exists random coupling from the fundamental mode to higher-order modes and vice versa because of fiber irregularities. This leads to the generation and propagation of a multitude of copies of the signal waveform across the fiber link. Due to modal dispersion, these signal copies propagate at various group velocities and interfere, either constructively or destructively, with the main signal propagating on the fundamental mode. This effect is referred to as multipath interference (MPI) [25], [22]. For modeling the impact of MPI-induced crosstalk, we assume that the QSMFs under consideration exhibit weak coupling between the fundamental mode group LP₀₁ and the higherorder mode group LP₁₁. For engineering purposes, we assume that MPI can be modeled as independent, zero-mean, complex Gaussian noises with a good degree of accuracy. Then, the MPI coefficient $\hat{\beta}$ in (1) can be calculated using power coupledmode theory [22].

B. Monte Carlo simulation results

Fig. 1 shows the variation of Q—factor as a function of the launch power per channel for different fiber configurations, where the QSMF length per span is varied in the range 0–100 km in steps of 5 km. Lines represent least-squares fit of Monte Carlo simulation data with (1). To distinguish various simulation cases, we identify individual traces with different colors: fiber configurations with QSMF in the range 0–45 km are shown in pink and the remaining configurations for QSMF in the range 45–100 km per span are shown in cyan. We highlight the extreme cases for 0 km, 45 km, and 100 km using thick red, black, and blue lines respectively.

We observe that the optimum Q-factor increases as the QSMF length per span is increased up to 45 km. For QSMF segments longer than 45 km, the optimum Q-factor gradually declines, eventually reaching a 0.4 dB decrease at 100 km from the peak performance achieved at 45 km.

C. Analytical model validation

Since it is cumbersome to display both the analytical model and the numerical data on the same graph, we shall hereafter focus only on the extreme cases for 0 km, 45 km, and 100 km of the above graph. Then, we replot the Q-factor against the average launch power as given by the Monte Carlo simulation for three different configurations of QSMF and SMF (Fig. 2),

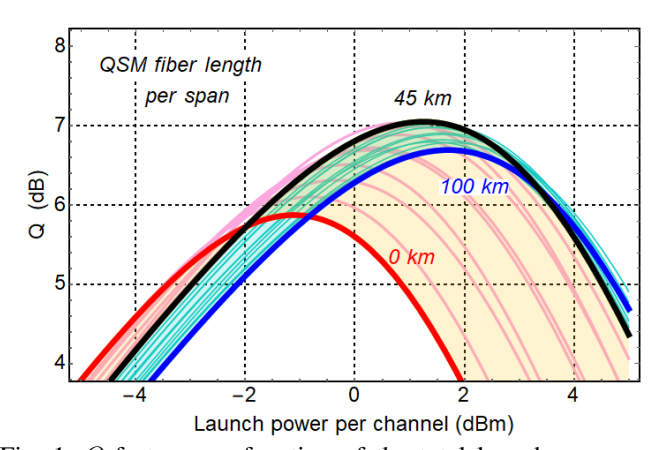


Fig. 1: Q-factor as a function of the total launch power per channel for different QSMF lengths per span. (Conditions: System length: 6,000 km, 100 km spans, QSMF effective mode area: 250 μ m², SMF effective mode area: 112 μ m². No MPI compensation. Lines: Fitting using (1).)

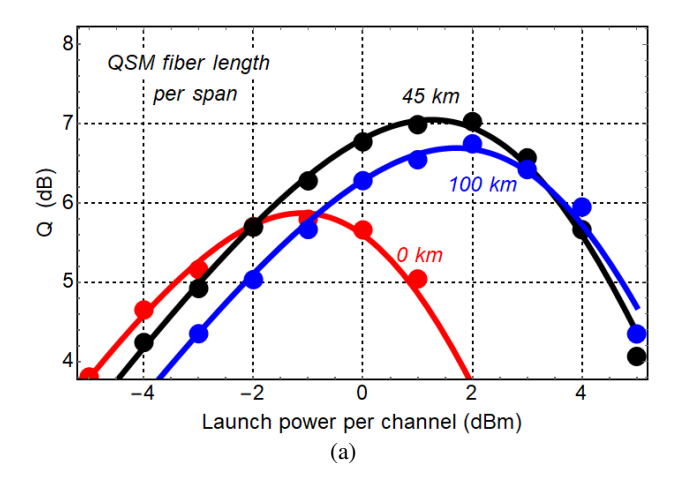
i.e., using only SMF (in red), only QSMF (in blue), and a 45/55 mix of QSMF and SMF (in black). We distinguish two cases:

- (a) 0% MPI compensation at the coherent receiver (Fig. 2a): The optimum Q-factor increases from 5.9 dB for SMF to 7 dB for 45/55 mix of QSMF and SMF and then drops to 6.7 dB for QSMF only. In this specific case, the optimum Q-factor is maximized with the use of 45 km QSM fiber per span. The Q-factor improvement for using hybrid fiber spans compared to using SMF exclusively is 1.2 dB.
- (b) 100% MPI compensation (Fig. 2b): The optimum Q-factor increases from 5.9 dB for SMF, to 7.5 dB for 45/55 mix of QSMF/SMF, to 7.8 dB for QSMF only. In this specific case, the optimum Q-factor is maximized with the exclusive use of QSMF per span. The Q-factor improvement for using only QSMF as opposed to using SMF exclusively is 1.9 dB.

The lines in Fig. 2 are obtained by least squares fitting of the numerical results using (1). Notice that the numerical results and the fitted lines agree extremely well and this is a strong indication that (1) is indeed an accurate model. However, the analytical calculation of $\tilde{\gamma}$ in (1) from first principles using the proposed nonlinear GN model is rather inaccurate.

1) Q vs. P curves: Next, we check the accuracy of the proposed nonlinear GN model against Monte Carlo simulation. We will show that the proposed nonlinear GN model describes qualitatively the general shape of the simulated Q vs. P curves but it does not provide pointwise accuracy. Nevertheless, as we are going to see subsequently, despite its quantitative errors, the proposed nonlinear GN model is sufficient for a quick determination of the optimum fiber splitting ratio.

As an illustration of the disagreement between the proposed nonlinear GN model and the simulation results, we replot from Fig. 2a the Monte Carlo simulation points (circles) describing



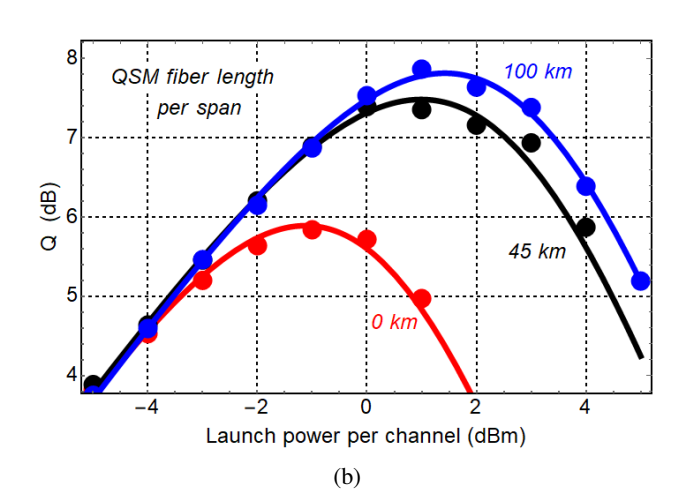


Fig. 2: Q-factor as a function of the total launch power per channel. (a) No MPI compensation; (b) 100% MPI compensation. (Symbols: Points: Monte Carlo simulations; Lines: Fitting using (1).)

the variation of the Q-factor as a function of the average launch power for the case of 45/55 QSMF/SMF mix in the absence of MPI compensation (Fig. 3).

On the same graph, we superimpose the incoherent nonlinear GN model with $\epsilon=0$ (in blue), the coherent nonlinear GN model (in red), and the partially-coherent nonlinear GN model with $\epsilon=0.15$ (in black). The analytical models based on coherent and incoherent addition deviate from the numerical results at relatively small launch powers. The peak deviation of the analytical curves in blue and red from the numerical results varies with the fiber attributes and system parameters. In this particular case, if we compare the values at the maxima, there is a mismatch of 0.4 dB between the coherent nonlinear GN model and the simulation. The discrepancy between the analytical and numerical results can be remedied to some extent by using the partially-coherent nonlinear GN model with ϵ as a fitting parameter (black line).

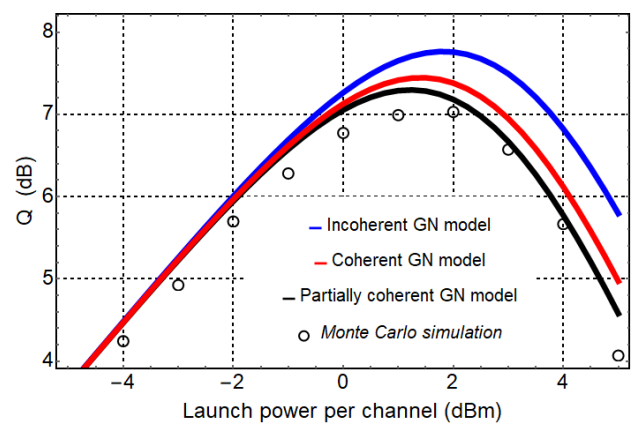


Fig. 3: *Q*-factor as a function of the total launch power per channel for 45/55 QSMF/SMF mix. (Condition: No MPI compensation.)

2) Optimum Q-factor vs. QSMF length: As another illustration of the validity of the analytical model, we examine the variation of the peak Q-factor Q_0 as a function of the QSMF length per span (Fig. 4). A major disagreement is apparent. However, we notice that the optimum QSMF length, where the peak Q-factor Q_0 occurs, does not differ substantially from curve to curve. The fact that we obtain essentially the same predictions for the optimum QSMF length from all the different variants of the analytical model is indicative of its usefulness.

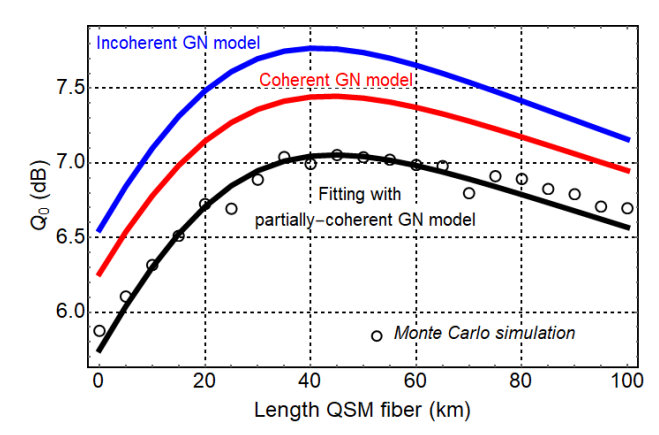


Fig. 4: Peak Q-factor Q_0 vs. QSMF length ℓ_{s_1} per span. (Condition: No MPI compensation.)

3) Optimum splitting ratio vs. MPI compensation: Fig. 5 shows a plot of the optimum splitting ratio vs. MPI compensation. The vertical axis is normalized so that the span length ratio varies between zero and one. Monte Carlo simulation data are represented by blue points. The blue line shows a phenomenological model fit of the Monte Carlo simulation data. The blue shaded region around the blue line indicates ± 0.1 dB deviations from the optimum Q-values. The other lines show the predictions of different variants of the modified nonlinear GN model. As the MPI compensation increases, the

ratio ℓ_{s_1}/ℓ_s increases to unity. The modified nonlinear GN model predictions are within the blue region.

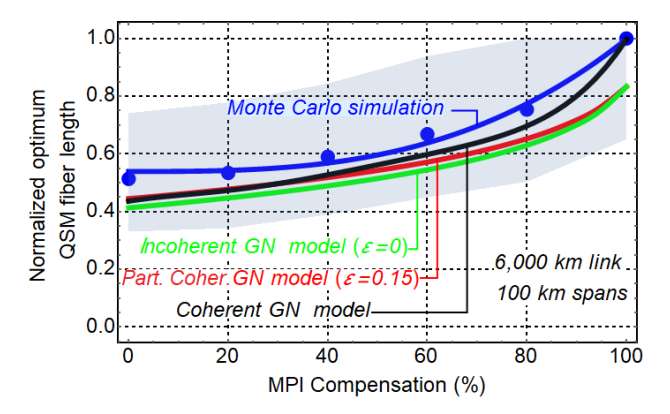


Fig. 5: Variation of the optimal normalized QSMF length per span ℓ_{s_1}/ℓ_s as a function of the percentage of MPI compensation at the coherent optical receiver.

Besides these validity checks, there are others presented by the authors at ECOC'17 [19] for different fiber parameters that corroborate the current findings. Therefore, we believe that we have established the validity of the proposed analytical model for the practical determination of the optimum fiber splitting ratio per span. Henceforth, instead of numerically optimizing the lengths of the different fiber segments per span by solving the Manakov equation, which is a time consuming process, one can conveniently resort to the analytical model.

IV. SUMMARY

The nonlinear GN model is a well-established theoretical framework based on a set of simplifying hypotheses ensuring mathematical tractability. The conventional nonlinear GN model was developed for uniform fiber spans. Here, we generalized its formalism to the case of hybrid fiber spans. We performed extensive Monte Carlo simulation verification for a representative transatlantic point-to-point link of total length equal to 6,000 km with 100 km hybrid fiber spans, composed of an experimental QSMF and a commercially-available, ultra-low-loss, large-effective-area SMF without any splice losses. We showed that the modified nonlinear GN model is sufficiently accurate for the determination of the optimum fiber splitting ratio per span, yielding a system performance within ± 0.1 dB from the optimum Q-value.

REFERENCES

- [1] G. P. Agrawal, Nonlinear Fiber Optics, 5th ed. Academic Press, 2012.
- [2] P. K. A. Wai and C. R. Menyuk, "Polarization mode dispersion, decorrelation, and diffusion in optical fibers with randomly varying birefringence," *J. Lightw. Technol.*, vol. 14, no. 2, pp. 148–157, Feb. 1006
- [3] X. Chen and W. Shieh, "Closed-form expressions for nonlinear transmission performance of densely spaced coherent optical OFDM systems," Opt. Express, vol. 18, no. 18, pp. 19 039–19 054, Aug. 2010.
- [4] W. Shieh and X. Chen, "Information spectral efficiency and launch power density limits due to fiber nonlinearity for coherent optical ofdm systems," *IEEE Photonics Journal*, vol. 3, no. 2, pp. 158–173, April 2011.

- [5] P. Poggiolini, A. Carena, V. Curri, G. Bosco, and F. Forghieri, "Analytical modeling of nonlinear propagation in uncompensated optical transmission links," *IEEE Photon. Technol. Lett.*, vol. 23, no. 11, pp. 742–744, June 2011.
- [6] A. Carena, V. Curri, G. Bosco, P. Poggiolini, and F. Forghieri, "Modeling of the impact of nonlinear propagation effects in uncompensated optical coherent transmission links," *J. Lightw. Technol.*, vol. 30, no. 10, pp. 1524–1539, May 2012.
- [7] P. Poggiolini, "The GN model of non-linear propagation in uncompensated coherent optical systems," *J. Lightwave Technol.*, vol. 30, no. 24, pp. 3857–3879, Dec. 2012.
- [8] P. Johannisson and M. Karlsson, "Perturbation analysis of nonlinear propagation in a strongly dispersive optical communication system," J. Lightw. Technol., vol. 31, no. 8, pp. 1273–1282, 2013.
- [9] P. Poggiolini, G. Bosco, A. Carena, V. Curri, Y. Jiang, and F. Forghieri, "The GN-model of fiber non-linear propagation and its applications," *J. Lightwave Technol.*, vol. 32, no. 4, pp. 694–721, Feb. 2014.
- [10] A. Mecozzi and R.-J. Essiambre, "Nonlinear Shannon limit in pseudolinear coherent systems," *J. Lightw. Technol.*, vol. 30, no. 12, pp. 2011–2024, 2012.
- [11] R. Dar, M. Feder, A. Mecozzi, and M. Shtaif, "Properties of nonlinear noise in long, dispersion-uncompensated fiber links," *Opt. Express*, vol. 21, no. 22, pp. 25 685–25 699, Nov. 2013.
- [12] A. Carena, G. Bosco, V. Curri, Y. Jiang, P. Poggiolini, and F. Forghieri, "EGN model of non-linear fiber propagation," *Opt. Express*, vol. 22, no. 13, pp. 16335–16362, Jun. 2014.
- [13] P. Serena and A. Bononi, "A time-domain extended Gaussian noise model," J. Lightw. Technol., vol. 33, no. 7, pp. 1459–1472, 2015.
- [14] A. Ghazisaeidi, "A theory of nonlinear interactions between signal and amplified spontaneous emission noise in coherent wavelength division multiplexed systems," *J. Lightwave Technol.*, vol. 35, no. 23, pp. 5150– 5175, Dec. 2017.
- [15] V. Curri, A. Carena, P. Poggiolini, G. Bosco, and F. Forghieri, "Extension and validation of the GN model for non-linear interference to uncompensated links using raman amplification," *Opt. Express*, vol. 21, no. 3, pp. 3308–3317, Feb. 2013.
- [16] D. Semrau, R. I. Killey, and P. Bayvel, "The Gaussian noise model in the presence of inter-channel stimulated Raman scattering," *J. Lightw. Technol.*, vol. 36, no. 14, pp. 3046–3055, 2018.
- [17] H. Rabbani, G. Liga, V. Oliari, L. Beygi, E. Agrell, M. Karlsson, and A. Alvarado, "A general analytical model of nonlinear fiber propagation in the presence of Kerr nonlinearity and stimulated Raman scattering," arXiv e-prints, Sep. 2019, paper arXiv:1909.08714.
- [18] J. D. Downie, M. Mlejnek, I. Roudas, W. A. Wood, A. Zakharian, J. E. Hurley, S. Mishra, F. Yaman, S. Zhang, E. Ip, and Y. K. Huang, "Quasi-single-mode fiber transmission for optical communications," *IEEE J. Sel. Top. Quantum Electron.*, vol. 23, no. 3, pp. 1–12, May 2017.
- [19] L. Miranda, I. Roudas, J. D. Downie, and M. Mlejnek, "Performance of coherent optical communication systems with hybrid fiber spans," in *Eur. Conf. Opt. Commun. (ECOC)*, Gothenburg, Sweden, Sept. 2017, paper P2.SC6.18.
- [20] M. A. Z. Al-Khateeb, M. A. Iqbal, M. Tan, A. Ali, M. McCarthy, P. Harper, and A. D. Ellis, "Analysis of the nonlinear Kerr effects in optical transmission systems that deploy optical phase conjugation," *Opt. Express*, vol. 26, no. 3, pp. 3145–3160, Feb. 2018.
- [21] L. Krzczanowicz, M. A. Z. Al-Khateeb, M. A. Iqbal, I. Phillips, P. Harper, and W. Forysiak, "Performance estimation of discrete Raman amplification within broadband optical networks," in *Opt. Fiber Commun. Conf. (OFC)* 2019, San Diego, CA, 2019, paper Tu3F.4.
- [22] M. Mlejnek, I. Roudas, J. D. Downie, N. Kaliteevskiy, and K. Koreshkov, "Coupled-mode theory of multipath interference in quasi-single mode fibers," *IEEE Photon. J.*, vol. 7, no. 1, pp. 1–16, Feb. 2015.
- [23] J. D. Downie, M.-J. Li, M. Mlejnek, I. G. Roudas, W. A. Wood, and A. R. Zakharian, "Optical transmission systems and methods using a QSM large-effective-area optical fiber," Dec. 12 2017, US Patent 9,841,555.
- [24] M.-J. Li, S. K. Mishra, M. Mlejnek, W. A. Wood, and A. R. Zakharian, "Quasi-single-mode optical fiber with a large effective area," Dec. 19 2017, US Patent 9,846,275.
- [25] Q. Sui, H. Zhang, J. D. Downie, W. A. Wood, J. Hurley, S. Mishra, A. P. T. Lau, C. Lu, H.-Y. Tam, and P. K. A. Wai, "Long-haul quasisingle-mode transmissions using few-mode fiber in presence of multipath interference," *Opt. Express*, vol. 23, no. 3, pp. 3156–3169, Feb. 2015